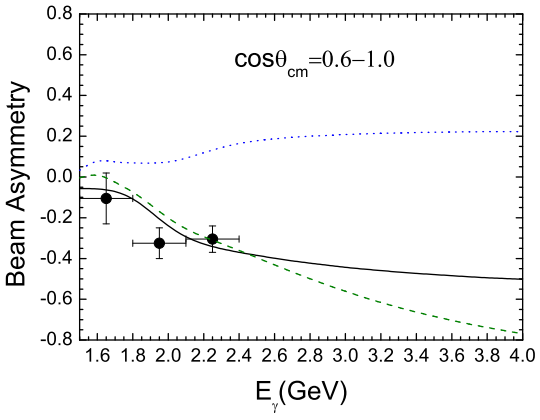

FIG. 4: The linear beam asymmetry for $\gamma + n \to K^+ + \Sigma^{(*)-}$ with $\cos\theta_{\rm c.m.}$ integrated from 0.6 to 1. Results of scheme I (solid curve), and scheme II (dashed curve) are compared with the LEPS data [9]. The dotted curve demonstrate the result with $h = 1$ and without $\Sigma(\frac{1}{2}^-)$ contribution.

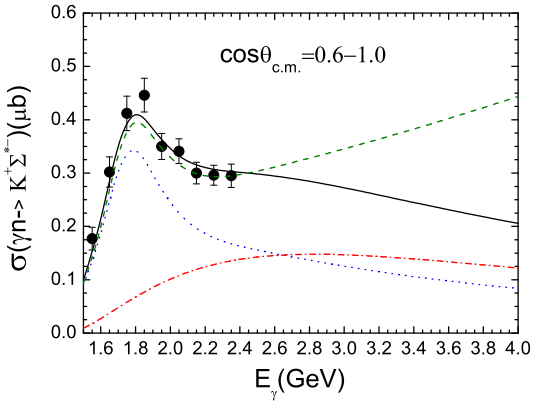

FIG. 5: Integrated cross sections for $\gamma + n \to K^+ + \Sigma^{(*)-}$ with $\cos\theta_{\rm c.m.} = 0.6 - 1.0$ of scheme I (solid curve) and scheme II (dashed curve), compared with the LEPS data [9]. The dotted and dot-dashed curves demonstrate the contributions from $\Sigma^*(\frac{3}{2}^+)$ and $\Sigma(\frac{1}{2}^-)$, respectively, in the scheme I.

rameter h to a larger value as scheme II can also have such an effect. The χ^2 for the two schemes are 97 and 102, respectively, compared to the 39 experimental data points in Figs. 3 & 4. As a comparison, the corresponding previous theoretical prediction [9] without including the two new ingredients give a χ^2 value about 180.

From the comparison of the results with the LEPS data, one can not tell for sure which one of the two schemes is better. In fact, some other combinations of h and $g_{KN\Sigma}$, such as $h = 1.06$ combined with $g_{KN\Sigma} = 1.04$, may also describe the present data. However, one can

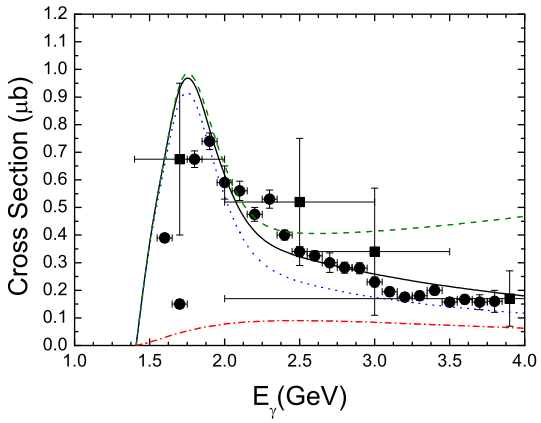

FIG. 6: Total cross sections for $\gamma + p \to K^+ + \Sigma^{(*)0}$ of scheme I (solid curve) and scheme II (dashed curve), compared with the CLAS preliminary data [2]. The dotted and dot-dashed curves demonstrate the contributions from $\Sigma^*(\frac{3}{2}^+)$ and $\Sigma(\frac{1}{2}^-)$, respectively, in the scheme I.

see from Fig. 5 that for higher incident energy, the two schemes give very distinctive predictions. Thus the schemes and mechanisms can be distinguished when data on reaction $\gamma n \to K^+\Sigma^{*-}$ at higher incident energies are available.

The above results show that while the original theoretical prediction with $\Sigma^*(\frac{3}{2}^+)$ production alone with $h = 1$ fails to reproduce the data for $\gamma n \to K^+\Sigma^{*-}$ [9, 12], the data can be well reproduced either by increasing h to 1.11 or by including an additional $\Sigma(\frac{1}{2}^-)$ resonance around 1380 MeV. Since the parameters for the original theoretical prediction come from the fits to the data on the $\gamma p \to K^+\Sigma^{*0}$ process, we need to check how the new sets of parameters fit to the $\gamma p \to K^+\Sigma^{*0}$ data. The results are shown in Fig. 6 for the total cross sections of the reaction $\gamma p \to K^+\Sigma^{*0}$ with the above sets of parameters, comparing with the CLAS data [2]. Again, the solid line is the result for $\Sigma^*(\frac{3}{2}^+)$ production with $h = 1$ combined with the contribution from $\Sigma(\frac{1}{2}^-)$ with $g_{KN\Sigma} = 1.34$; the dotted line and the dashed line are the results for $\Sigma^*(\frac{3}{2}^+)$ production alone with $h = 1$ and $h = 1.11$, respectively. The $\Sigma(\frac{1}{2}^-)$ contribution is also shown by the dash-dotted line with $g_{KN\Sigma} = 1.34$. From Fig. 6 one sees that the combined result of $\Sigma^*(\frac{3}{2}^+)$ production with $h = 1$ and the $\Sigma(\frac{1}{2}^-)$ production (scheme I, solid line) can be compatible with the CLAS data on the whole, while the results with $h = 1.11$ (dashed line) deviate from the data for larger incident energy.

Our results show that the combined results of $\Sigma^*(\frac{3}{2}^+)$ and $\Sigma(\frac{1}{2}^-)$ production (solid line) can be compatible with both the $\gamma n \to K^+\Sigma^{*-}$ reaction data and the $\gamma p \to K^+\Sigma^{*0}$ reaction data with the same set of parameters